International Journal of GEOMATE, June, 2024 Vol.26, Issue 118, pp.17-24
ISSN: 2186-2982 (P), 2186-2990 (O), Japan, DOI: https://doi.org/10.21660/2024.118.4098
Geotechnique, Construction Materials and Environment

SIMULATION OF EARTHQUAKE INTENSITY FOR TSUNAMI PREDICTION AND DISASTER RISK MANAGEMENT

*Yusran Asnawi[1], Muhammad Gunaya[2], Suko Prayitno[3], Andrean Simanjuntak[2,3], Umar Muksin[2,4]

[1]Department of Science, Faculty of Science and Technology, Universitas Islam Negri Ar-Raniry, Indonesia
[2] Tsunami Disaster and Mitigation Research Center, Universitas Syiah Kuala, Indonesia
[3]State School for Meteorology Climatology and Geophysics (STMKG), Jakarta, Indonesia
[4]Department of Physics, Faculty of Mathematics and Natural Sciences, Universitas Syiah Kuala, Indonesia

*Corresponding Author, Received: 19 Aug. 2023, Revised: 13 April 2024, Accepted: 23 April 2024

ABSTRACT: On January 15, 2023, a major earthquake with Mw 6.2 occurred in the northern part of Sumatra, Indonesia, and generated widespread ground shaking around III – V MMI without any damages. The hypocenter was located at a shallower depth than the common slab contour, which may address another blind tectonic system called backthrust. An extended waveform inversion and hypocenter relocation analysis is demonstrated to identify the responsible system. A total of 1,750 earthquakes were compiled from the 10-year catalog (2010 – 2022) and recorded by 72 stations associated with 1,2536 P-phase and 5,604 S-phase. Up to 85% (1211) of the total earthquakes were successfully relocated, while 15% (103) were not relocated because they did not meet the predetermined criteria. Furthermore, the mainshock was resolved with a thrusting fault with NW – SE orientation, steeply dipping to the SW direction, and a moment magnitude estimation of Mw 6.2 ± 0.03 at a depth of 35.50 ± 2 Km. The focal parameters include two nodal planes, i.e., the 1st nodal plane with strike 319°, dip 15.5°, and rake 101° while the 2nd nodal plane with strike 127°, dip 74.8° and rake 86.8°. The results successfully show the existence of the blind back thrust in the Sumatra subduction zone, which will provide new insight and contribute to the recent tectonic system in the northern part of Sumatra and its surroundings.

Keywords: Earthquake, Backthrust, Hypocenter Relocation, Moment Tensor, Subduction, Tectonic

1. INTRODUCTION

On January 15, 2023, a major earthquake with Mw 6.2 occurred suddenly in the northernmost part of Sumatra. The Indonesia Meteorological Geophysical and Climatology Agency (BMKG) reported that the earthquake generated significant ground shaking around III – V MMI without any damages. Several agencies (USGS, GFZ, GCMT, and IPGP) released information that the earthquake occurred with a thrusting mechanism while striking in a NW-SE direction, which is parallel with the subduction line. The thrusting mechanism suggests a possible connection with the subduction process. However, the location and depth of the earthquake occurred at a shallower depth than the common slab contour, which may address another possible tectonic system.

Tectonically, Sumatra Island is categorized as an earthquake-prone area due to its location in the megathrust region. The megathrust earthquake occurred potentially as the consequence of the subduction of the Indo-Australian plate beneath the Eurasian plate with 5 - 6 cm/yr with a dipping angle of 40 - 50° [1,2]. Seismically, the northern part of Sumatra is located on the active tectonic system (Fig.1) and consequently generates several major earthquakes such as 2004 Sumatra-Andaman Mw 9.0 [3], 2005 Nias Mw 8.5 [4], and 2012 Double-let earthquake in the Wharton Basin with Mw 8.2 and Mw 8.1 [5]. Meanwhile, the historical land earthquakes are generated by several active segmentations in the Sumatra Fault System with a slip rate of 10-20 mm/yr [6,7]. The historical events are, e.g., 1964 Seulimeum Mw 6.4 [7], 1996 Kutacane Mw 6.1 [5], 2013 Bener Meriah Mw 6.3 [6], and 2017 Pidie Jaya Mw 6.5 [7]. Moreover, in Sumatra, in the last decade, there has been no major earthquake larger than Mw 8.0. On the other hand, there is less information and fewer studies about the seismic activities from the back thrust system in the subduction zone.

Several studies have aimed to explain the backthrust system in the Sumatra tectonic process, e.g., Chauhan et al. [8] used seismic tomography to determine the possibility of uplifting along the backthrust branches that can influence the formation of the forearc islands along the trench of the northern part of Sumatra Island. Those authors also assume that the back thrust system can co-seismically slip during megathrust events, and it is possible to generate a significant tsunami and seismic hazard in the region. However, Singh et al. [9] determined evidence for the active backthrust with a southwest dip direction in the northeastern part of Mentawai Island. The backthrust system in the megathrust zone can provide new insight that

can be used to study the forearc formation along the trench line of offshore Sumatra Island.

Several multidisciplinary studies have been conducted in the northern part of Sumatra, such as seismic hazard and microzonation [6,10,11], detail of active fault [12, 13], geodetic mapping [4], and tsunami modeling [3]. Meanwhile, no study has defined the backthrust system using recent seismicity. Therefore, we present the seismic analysis combining the waveform inversion and hypocenter relocation to figure out the backthrust system.

2. RESEARCH SIGNIFICANCE

The results successfully show the existence of the backthrust system in the Sumatra subduction zone. The presence of the backthrust can be used to analyze future similar earthquakes. The results will provide new insight and contribution to the recent tectonic system in the northern part of Sumatra and its surroundings.

3. MATERIALS AND METHODS

3.1 Seismic Data and Hypocenter Relocation

Two types of seismic data, including the seismic waveform of the mainshock and the seismic phase arrival times (P and S phases), were utilized to describe the tectonic process of the earthquake. The Meteorology, Climatology, and Geophysics Agency (BMKG, Indonesia) has been recording the arrival timings at each permanent seismic station for the past ten years. Here, the earthquake hypocenter is crucial to determine a specific cluster using the seismic arrival time.

The earthquake criteria were established as follows: the total of seismic phases was set at 10 with a minimum of 4 S-phases; the depth range for the hypocenter must be between 0 and 200 km; the azimuth gap coverage below 200°; and the separation between hypocenters with station distribution must be between 0 and 4°. Based on these criteria given, a total of 1,750 earthquakes

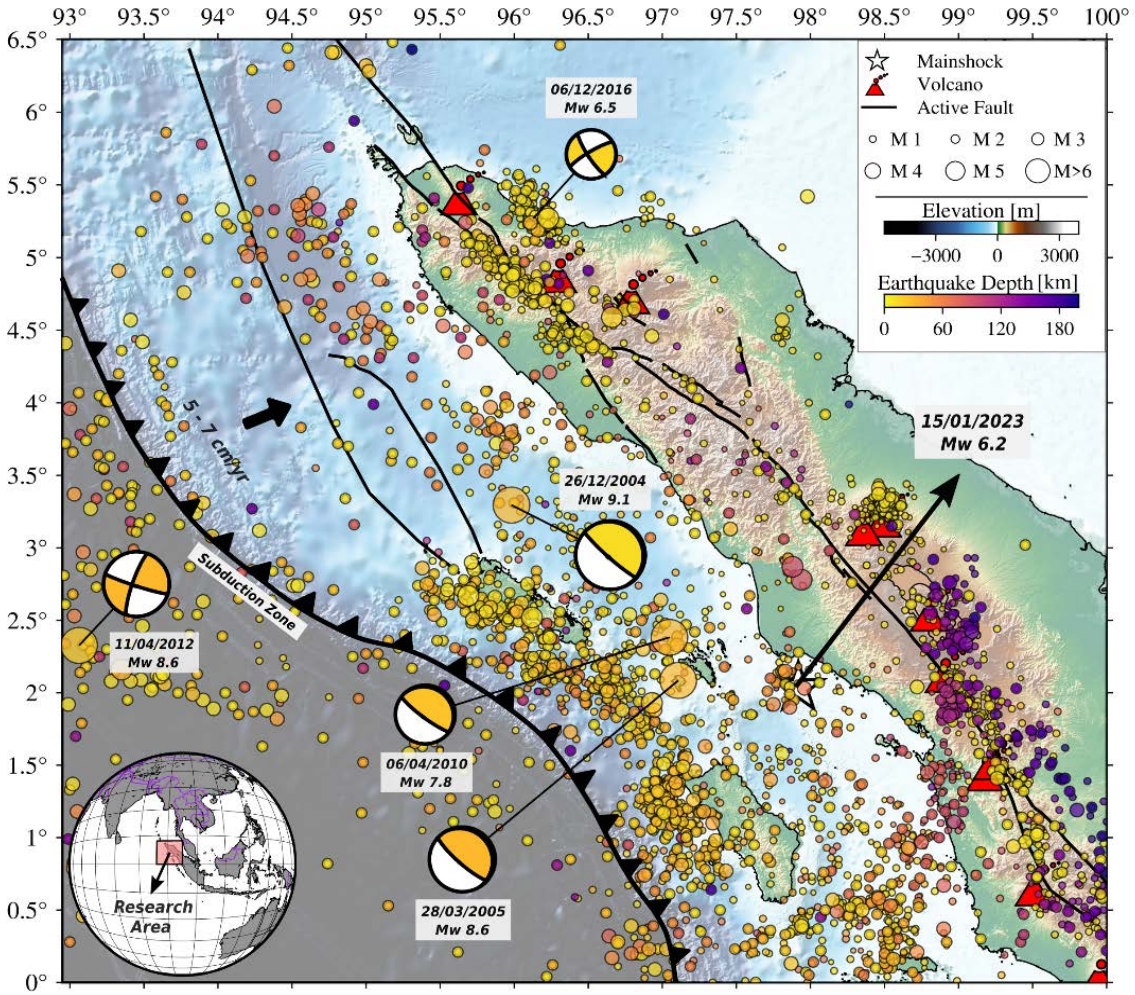

Fig. 1 Tectonic map of the northern part of Sumatra Island shows the current seismicity with the focal mechanisms over the last two decades and the latest earthquake on 2023 with Mw 6.2 (white star).

from the 10-year catalog database (2012 – 2022) that were captured by 72 stations were obtained (Fig. 2). In total, 12,536 P-phase and 5,604 S-phase as the body-wave seismic phases were collected for hypocenter relocation. To calculate the detailed structure that can be found from hypocenter relocation, precise earthquake location is required. Here, the hypocenter was clustered based on the relative displacement using the HypoDD program [14]. The fundamental method of HypoDD makes the assumption that if two earthquakes occur with hypocenter distances that are closer together than the distance to the recording station, their paths will have similar mediums. In an iterative process, HypoDD reduces the residual between the observed and calculated arrival time, as shown in Fig. 3. The hypocenter position will be updated following each iteration, and HypoDD minimizes the remaining time between the computed and observed values. The final hypocenters are grouped together by the residual time after relocation using the timing differences in each iteration.

3.2 Bayesian Moment Tensor Inversion

Using Bayesian moment tensor inversion for the mainshock, we analyzed the earthquake mechanism using seismic waveform data. The waveform data were collected from a seismic network with free access that is 1,000 km away from the epicenter (https://geofon.gfz-potsdam.de and http://ds.iris.edu/SeismiQuery/). The three rotating components (Z, Radial, and Transversal) were subjected to the inversion strategy utilizing the Grond probabilistic earthquake source inversion framework [15].

The Grond provides consideration of an uncertainty in the nonlinear model using the Bayesian estimation method and a bootstrap optimization. Until it is equal to or less than the continually estimated updates of the dispersed parameters, the distribution of newer models will be significantly improved based on the tested models.

4. RESULTS AND DISCUSSION

The hypocenter relocation processing used the velocity models from Simanjuntak et al. [10] that were derived from the study of the slab gap beneath

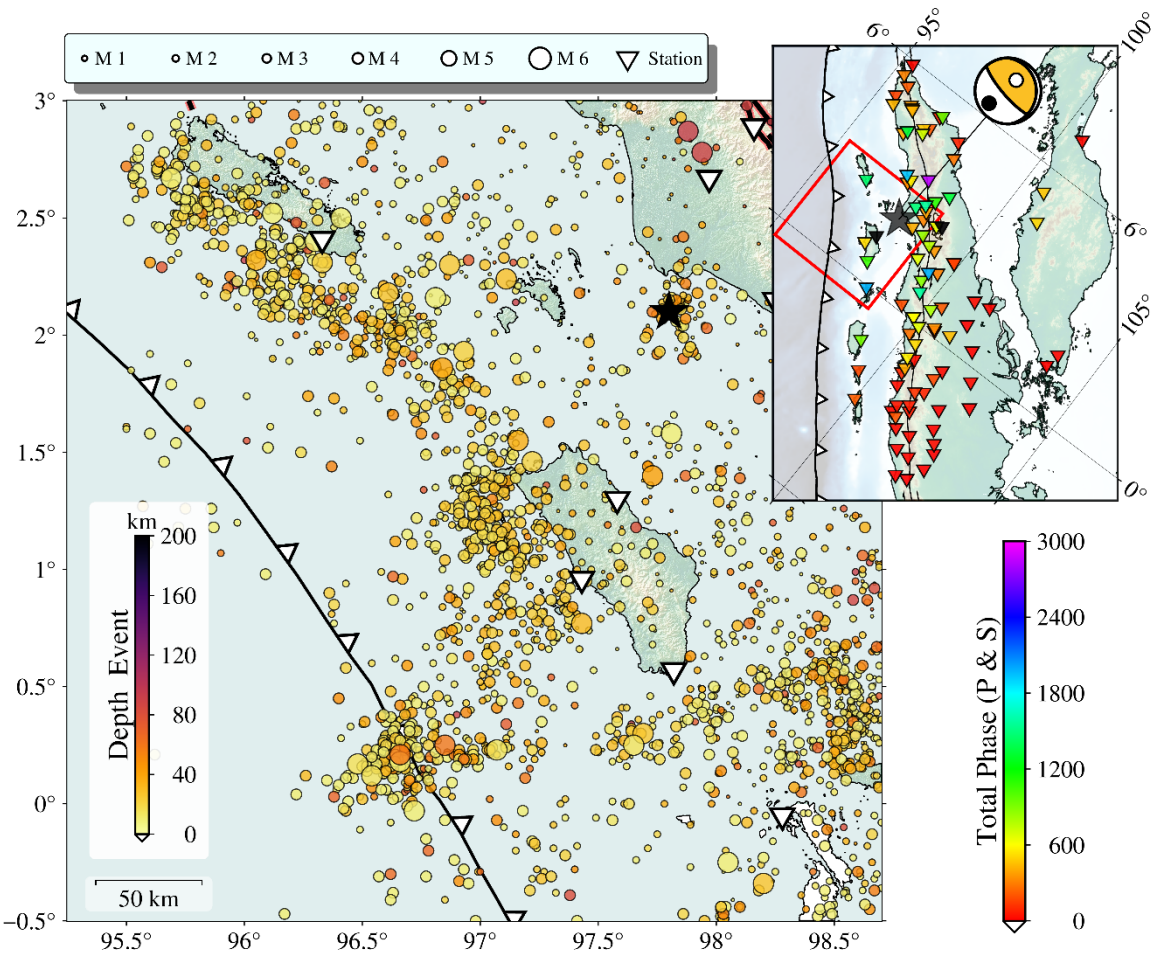

Fig. 2 Seismicity map shows epicenter distribution at depths in the range of 0-200 km. The recording stations are located at distances ranging from 0 to 5° (500 km), with a total range of P and S picks 0 to 3,000 picks.

Toba (Sumatra). The shifting hypocenter location and depth gives values in the range of 10 - 20%. The relocation results successfully gain the quality of the hypocenter and provide precise clusters.

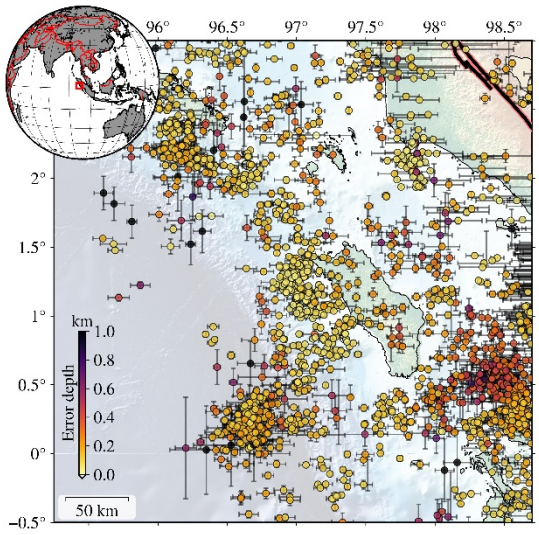

Fig. 3 The seismicity map after relocation with the ellipsoid error and depth (0 – 1 km) shows an adequate error in the geographical direction.

The relocation parameters were set with a maximum separation of 30 km, a maximum of 20 neighbors per event, and a minimum of 8 phases for connections needed to identify neighbors. Because it is more effective, the conjugate gradient for least-squares (CGLS) method was chosen to move a large number of earthquakes. Following Waldhauser [14], the damping parameter was adjusted at a value of 20 to produce a CND parameter between 40 and 80 for the bulk of the generated hypocenters. For each iteration, the relative positions of the hypocenters must be determined using a weighting factor because the original data have a standard deviation a priori. Finally, as many as 85% of the total number of earthquakes were successfully relocated, while 103 were not relocated. With an RMS of 0.2 to 0.8s, the relocation findings demonstrate a considerable shift in the hypocenter quality; almost 90% of all hypocenter relocations have RMS 0.5s, and 60% have RMS > 0.5s.

The mainshock was updated with a thrusting mechanism in the NW – SE striking direction with a moment magnitude estimation Mw of 6.2 ± 0.01 and depth of 35.50 ± 2 Km. For inversion, a Green's functions model from a pre-calculated velocity model was applied with fitted full displacement waveforms [15]. We applied a bandpass filter of 0.03 and 0.07 Hz for the mainshock. A total of 1,000 different configurations were given with 30,000 interactions to provide a final convergence solution. The deviatoric composition of the moment tensor results for the mainshock consists of a double couple (DC) component of 92 ± 1% and a Compensated Linear Vector Dipole (CLVD) component of 8 ± 1%.

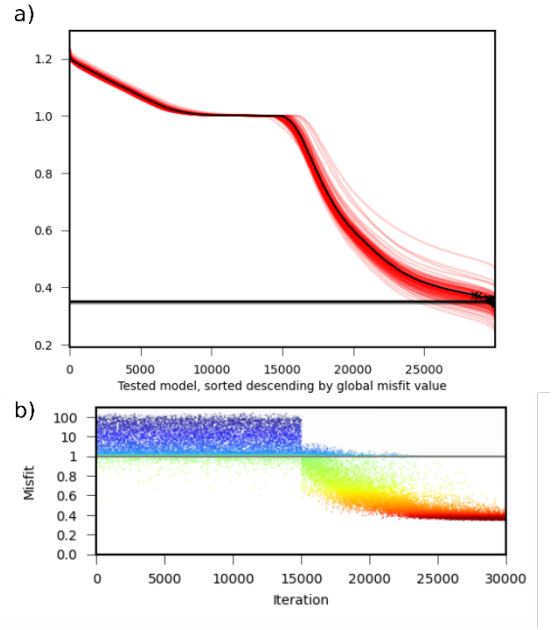

Fig. 4 Graph of tested models with the black line as the converged solution (a). Graph of misfit in each iteration shows the significant change of RMS after 30,000 iterations (b).

The focal parameters result contains two nodal planes i.e., 1st nodal plane with a strike of 319°, a dip of 15.5°, and a rake of 101° while the 2nd nodal plane has a strike of 127°, a dip of 74.8°, and a rake of 86.8° as shown in Fig. 5. The focal parameter results are well resolved with a satisfactory uncertainty for two nodal planes (± 2°) and adequate misfit < 0.5. The mainshock suggests a rupture propagation towards NW – SE that is parallel with the trench line and steeply dipping to the SW direction.

4.1 Seismicity Profile

To see the hypocenter distribution change in the vertical direction, we added a cross section aimed at resolving the seismicity in the vertical profile. An oblique line (A-A) was added to cross the dip angle of the focal mechanism result (2nd nodal plane) and combine with relocation results, as shown in Fig. 5. The cross section shows clusters that follow a subduction slab at a depth of 0 - 80 Km. The subduction gap is clearly described along the slab with low seismicity at the depths of 20 – 40 km and 60 – 80 km.

The low seismicity can be addressed by referring to an existing system along the forearc

island, such as Simeleu Island and Nias Island. The seismicity along the slab occurs mostly in the interface zone, which is the location of the potential megathrust earthquake. On the other hand, the low seismicity in the interface zone indicates a locking zone with the possibility of an asperity. In the southwestern part of Nias Island, another tectonic system called an outer rise shows a specific cluster at a shallow depth below 30 km that may be associated with normal faulting [16].

The vertical profile of the hypocenter relocation shows there is low seismicity after the forearc island that started at a depth of 20 until 80 km. The low seismicity can be linked to the blind system that generated the Mw 6.2. The hypocenter distribution clearly shows a thrusting system with an angle dip perpendicular to the slab subduction line. The thrusting system indicates an active backthrust beneath northeastern part of Nias Island and may be responsible for the Mw 6.2. However, a lack of research on the backthrust around the epicenter can be resolved by using the hypocenter and focal mechanism result.

4.2 Backthrust in Sumatra

The formation of the forearc islands along the northern Sumatra trench indicates a possible geological process, such as an uplifting phenomenon. The uplifting has been formed during the recent geological past, and it has uplifted co-seismically with the 2004 Mw 9.0 and 2005 Mw 8.5 occurrences [3,8,9,17]. Briggs et al. [17] studied the estimation of an uplift rate for Nias Island and its surroundings around ~0.5 mm/yr, indicating an active tectonic faulting. The deformation process on Nias Island with an uplifting may also favor the possibility of active backthrusting along the west coast of Sumatra that can be aseismic or co-seismic [4,8,18,19].

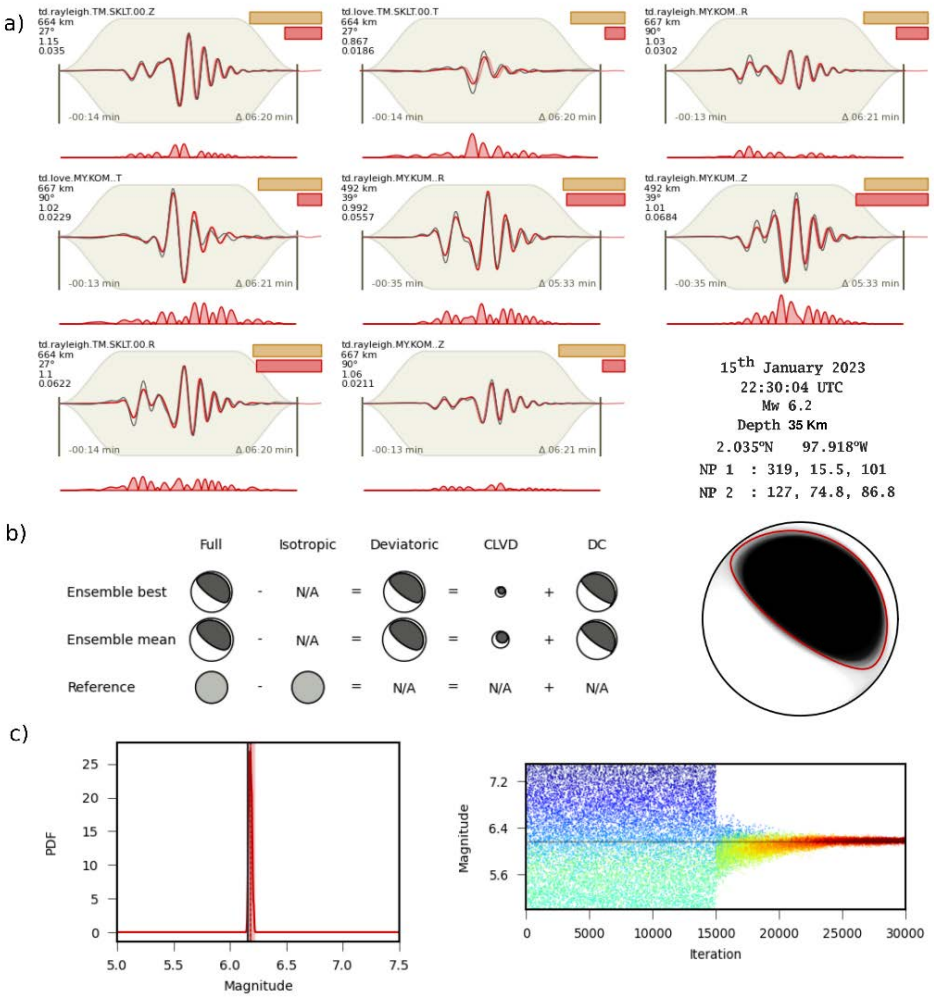

Fig. 5. Summaries of the moment tensor inversion results show the fitting waveform between observation (black line) and synthetic (red line) with focal spheres and graph of the probability density function (PDF).

The subduction process beneath Sumatra Island that formed uplifted, folded, and faulted sediments on the forearc ridge and basin can be used to explain the back thrust in the southwestern part of Aceh [20,21], as shown in the diagram in Fig. 7. Furthermore, Singh et al. [9] identified the backthrust system as the part of the geological structure that has resulting ridge-like features along the forearc system in the Sumatra trench line. The information for the backthrust system can be useful to conceptualize a further disaster mitigation plan [22-24]. On the other hand, the relationship between the spatial and temporal seismicity around the backthrust system is difficult to estimate due to poor bathymetric profile and no seismic reflection research close to the epicenter location.

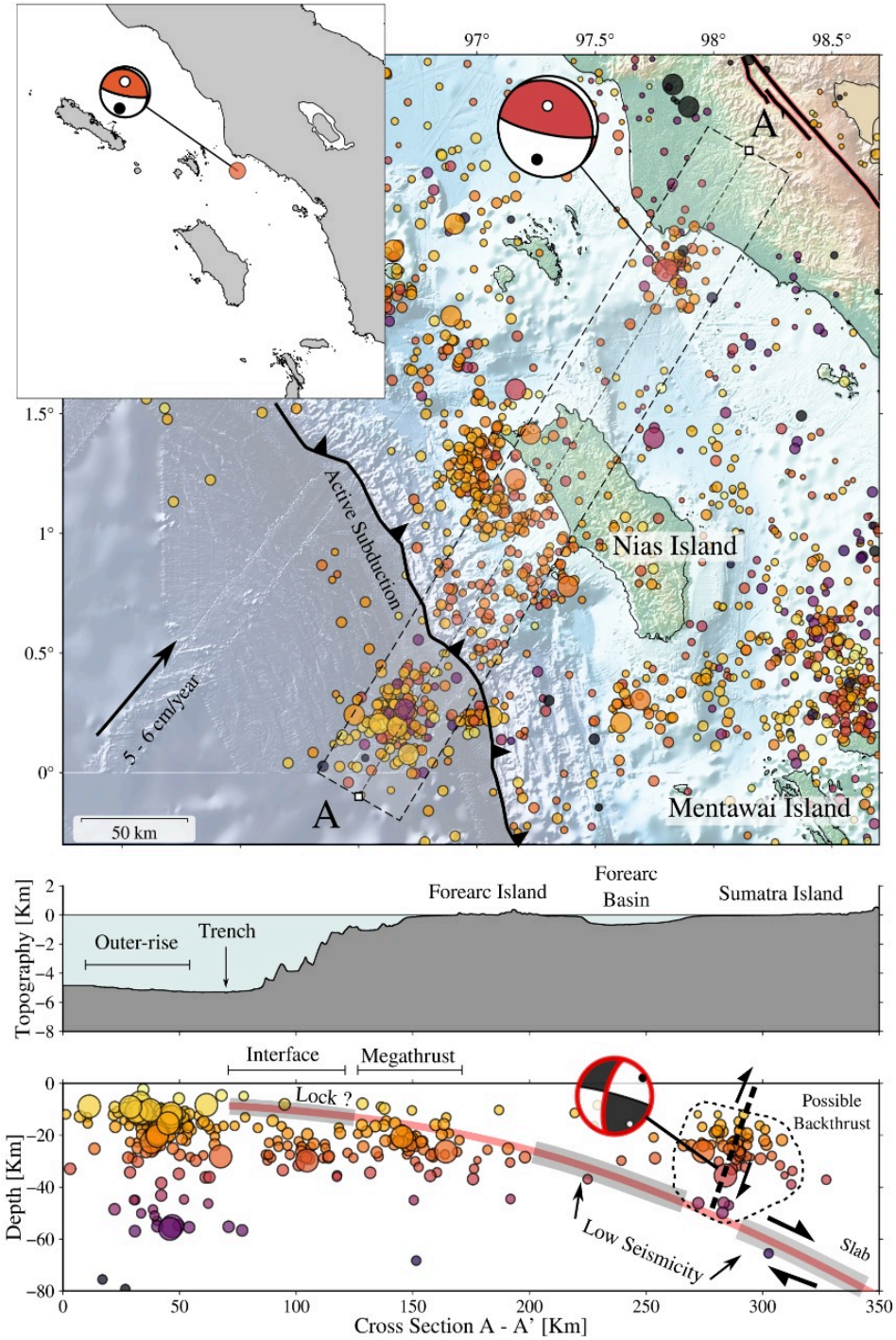

Fig. 6. Seismicity map after relocation shows specific clusters with cross-section profiles of A-A' slice. The vertical profiles show the backthrust dipping to the SE direction that is associated with the 2nd nodal plane.

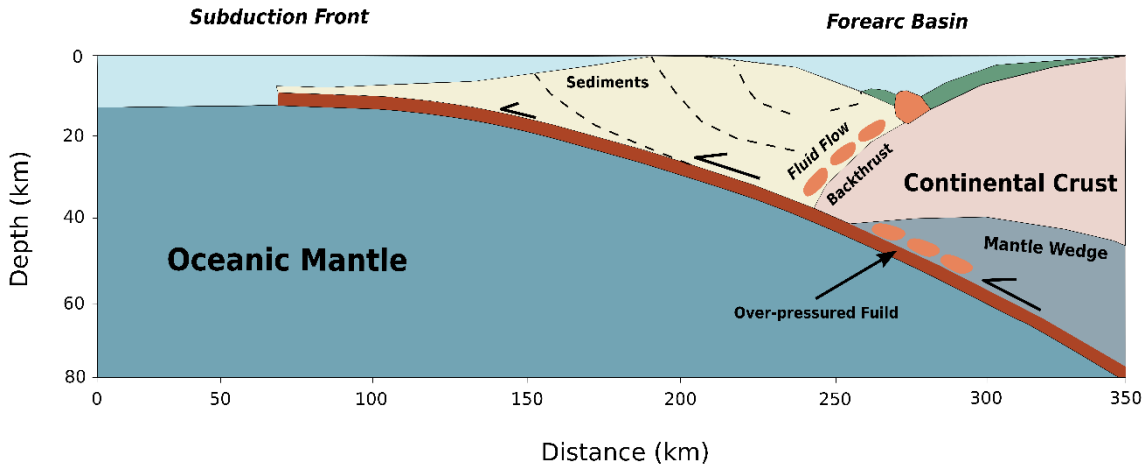

Fig. 7. Schematic cartoon shows a slab contour (red line) between the Indo-Australian plate towards beneath the Eurasian plate with several geodynamic processes.

However, the present research provides an initial indication of an active blind backthrust. Further investigation into the backthrust system must be conducted to provide a detailed understanding, especially for the recent tectonic system and structure.

5. CONCLUSIONS

This comprehensive analysis successfully defined the possibility of a back thrust system by combining the moment tensor inversion with hypocenter relocation to identify the fault responsible for generating an earthquake with M_w 6.2. In this study, 85% of the total earthquakes (~1500 events) were relocated with a thrusting fault with NW – SE orientation and M_w of 6.2 ± 0.03 at a depth of 35.50 ± 2 Km. The focal parameters include two nodal planes, i.e., 1st nodal plane has a strike of 319°, dip of 15.5°, and rake of 101° while the 2nd nodal plane has a strike of 127°, dip of 74.8°, and rake 86.8°. The source mechanism consists of a DC component of 92 % and a CLVD component of 8 %. The results successfully show the existence of the blind backthrust in the Sumatra active subduction zone system.

6. REFERENCES

[1] Prawirodirdjo L., McCaffrey R., Chadwell C. D., Bock Y., & Subarya C., Geodetic Observations of An Earthquake Cycle at The Sumatra Subduction Zone: Role of Interseismic Strain Segmentation, Journal of Geophysical Research: Solid Earth, Vol. 115, Issue B3414, 2010, pp. 1-15.

[2] Simanjuntak A. V. H., & Ansari K., Spatial Time Cluster Analysis and Earthquake Mechanism for Unknown Active Fault (Kalatoa Fault) in The Flores Sea. Earth Science Informatics Vol.7, Issue 1, 2023, pp. 131-145.

[3] Lay T., Kanamori H., Ammon C. J., Nettles M., Ward S. N., Aster R. C., & Sipkin S., The Great Sumatra-Andaman Earthquake of 26 December 2004. Science, Vol. 308, Issue5725, 2005, pp. 1127-1133.

[4] Hill E. M., Yue H., Barbot S., Lay T., Tapponnier P., Hermawan I., & Sieh K., The 2012 Mw 8.6 Wharton Basin Sequence: A Cascade of Great Earthquakes Generated by Near-Orthogonal, Young, Oceanic Mantle Faults. Journal of Geophysical Research: Solid Earth, Voi. 120, Issue 5, 2015. pp. 3723-374.

[5] Sieh K. & Natawidjaja D., Neotectonics of The Sumatran Fault, Indonesia, Journal of Geophysical Research: Solid Earth, Vol. 105, Issue 12, 2000, pp. 28295–28326.

[6] Pasari S., Simanjuntak A. V., Mehta A. & Sharma Y., A Synoptic View of The Natural Time Distribution and Contemporary Earthquake Hazards in Sumatra, Indonesia. Natural Hazards, Vol. 108, Issue 1, 2021, pp. 309-321.

[7] Muzli M., Umar M., Nugraha A. D., Bradley K. E., Widiyantoro S., Erbas K., & Wei S., The 2016 M w 6.5 Pidie Jaya, Aceh, North Sumatra, Earthquake: Reactivation of an Unidentified Sinistral Fault in a Region of Distributed Deformation. Seismological Research Letters, Vol. 89, Issue 5, 2018, pp. 1761-1772.

[8] Chauhan A. P., Singh S. C., Hananto N. D., Carton H., Klingelhoefer F., & Dessa J. X., Sumatra OBS Scientific Team. Seismic Imaging of Forearc Backthrusts at Northern Sumatra Subduction Zone. Geophysical Journal International, Vol. 179, Issue 3, 2009, pp. 1772-1780.

[9] Singh S. C., Carton H., Tapponnier P., Hananto N. D., Chauhan A. P., Hartoyo D., & Martin J., Seismic Evidence for Broken Oceanic Crust in the 2004 Sumatra Earthquake Epicentral Region. Nature Geoscience, Vol. 1, Issue 11, 2008, pp. 777-781.

[10] Simanjuntak A. V. H., Muksin U., Arifullah A., Lythgoe K., Asnawi Y., Sinambela M., & Wei S., Environmental Vulnerability Characteristics in an Active Swarm Region. Global Journal of Environmental Science and Management, Vol. 9, Issue 2, 2023, pp. 211-226.

[11] Asnawi Y., Simanjuntak A. V., Muksin U., Okubo M., Putri S. I., Rizal S., & Syukri M., Soil Classification in A Seismically Active Environment Based on Join Analysis of Seismic Parameters. Global Journal of Environmental Science and Management, Vol. 8, Issue 3, 2022, pp. 297-314.

[12] Muksin U., Riana E., Rudiyanto A., Bauer K., Simanjuntak A. V. H., & Weber M., Neural Network-Based Classification of Rock Properties and Seismic Vulnerability. Global Journal of Environmental Science and Management, Vol. 9, Issue 1, 2023, pp. 15-30.

[13] Muksin U., Arifullah A., Simanjuntak A. V., Asra N., Muzli M., Wei S., & Okubo M., Secondary Fault System in Northern Sumatra, Evidenced by Recent Seismicity and Geomorphic Structure. Journal of Asian Earth Sciences, 2023, pp. 105557.

[14] Waldhauser F., hypoDD—A Program to Compute Double-Difference Hypocenter Locations (hypoDD version 1.0-03/2001). US Geol. Surv. Open File Rep., Open-file report 01-113, 2001, pp. 1-25.

[15] Heimann S., Isken M., Kühn D., Sudhaus H., Steinberg A., Vasyura-Bathke H., Daout S., Cesca S., and Dahm T., Grond – A Probabilistic Earthquake Source Inversion Framework, GFZ Data Services, V.1.0, 2018, pp.1.

[16] Simanjuntak A., Muksin U., Asnawi Y., Rizal S., & Wei S., Recent Seismicity and Slab Gap Beneath Toba Caldera (Sumatra) Revealed Using Hypocenter Relocation Methodology. GEOMATE Journal, Vol. 23, Issue 99, 2022, pp. 82-89.

[17] Briggs R. W., Sieh K., Amidon W. H., Galetzka J., Prayudi D., Suprihanto, I., & Farr T. G., Persistent Elastic Behavior Above a Megathrust Rupture Patch: Nias Island, West Sumatra. Journal of Geophysical Research: Solid Earth, Vol. 113, Issue B12, 2008, pp. 1-28

[18] Vita-Finzi C., Neotectonics and The 2004 and 2005 Earthquake Sequences at Sumatra. Marine Geology, Vol. 248, Issue 1-2, 2008, pp. 47-52.

[19] Pasari S., Simanjuntak A. V., & Sharma Y., Nowcasting Earthquakes in Sulawesi Island, Indonesia. Geoscience Letters, Vol. 8, Issue 1, 2021, pp. 1-13.

[20] Pasari S., Simanjuntak A. V., Mehta A., & Sharma Y., The Current State of Earthquake Potential on Java Island, Indonesia. Pure and Applied Geophysics, Vol. 178, Issue 8, 2021, pp. 2789-2806.

[21] Simanjuntak A. V., & Ansari K., Seismicity Clustering of Sequence Phenomena in The Active Tectonic System of Backthrust Lombok Preceding The Sequence 2018 Earthquakes. Arabian Journal of Geosciences, Vol. 15, Issue 23, 2022, pp. 758-768.

[22] Supendi P., Rawlinson N., Prayitno B. S., Widiyantoro S., Simanjuntak A., Palgunadi K. H., & Arimuko A., The Kalaotoa Fault: A Newly Identified Fault that Generated the M w 7.3 Flores Sea Earthquake. The Seismic Record, Vol. 2, Issue 3, 2022, pp. 176-185.

[23] Simanjuntak A. V., Palgunadi K. H., Supendi P., Daryono D., Prakoso T. A., & Muksin U., New Insight on the Active Fault System in the Halmahera Volcanic Arc, Indonesia, Derived from the 2022 Tobelo Earthquakes. Seismological Research Letters, Vol. 94, Issue 6, 2023, pp. 2586-2594.